

## OVERALL CRYSTALLIZATION KINETICS OF PET

Edgar D. Zanotto and Luciana R. Zanotto  
DEMa-UFSCar- Sao Carlos (Brazil)  
Annamaria Celli- HIMONT- Ferrara (Italy)

The crystallization kinetics of PET were determined by DSC and Hot-Stage Microscopy- HSM. Two methods of analyses (Avrami intercepts vs. crystallization half-times,  $t_{1/2}$ ) were combined with different forms of the diffusion term; the Williams-Landel-Ferry (WLF), the Hoffman approximation and the experimental value of the activation energy for reptation. Good agreement was found between the surface energy,  $\sigma_e$ , calculated from DSC and HSM data, using the intercepts or  $t_{1/2}$ . The WLF value of  $\sigma_e$  was much higher than from the other transport terms.  $\sigma_e$  determined from the overall crystallization kinetics is close to  $\sigma_e$  from spherulitic growth rates.

PET, crystallization, kinetics, surface  
energy, Avrami, DSC

### 1. INTRODUCTION

Many properties of polymers strongly depend on the crystallinity and on crystal morphology. Thus, it is very important to understand and control the crystallization mechanisms and kinetics, as well as the physics of chain folding in these polymers. Poly(ethylene terephthalate)- PET- was chosen for this study because its crystallization rate is slow enough to be measured precisely in a wide temperature range.

Many studies of PET crystallization have been carried out. For instance, [1-6] determined the Avrami coefficients ( $n$ ) in wide temperature ranges. The values of  $n$  varied from 1 to 4 among the different papers, reflecting chemical and thermal history differences among the specimens, as well as in the techniques used. The crystallization half-lives,  $t_{1/2}$  vs.  $T$  curves have been reported by [2,5-9], among others. The most striking feature of these curves is the minimum time (maximum crystallization rate) at  $\sim 175-180^\circ\text{C}$ , independently of molecular weight and chemical purity, in all papers. Direct determinations of spherulitic growth rates have been performed by [10-12]. The maximum growth rates

also occur at  $175-180^\circ\text{C}$ .

The objectives of this work are:

- i) To determine quantitatively the overall crystallization kinetics by both differential scanning calorimetry (DSC) and hot stage microscopy (HSM);
- ii) to compare the kinetic results from a commonly employed approximate method (using  $t_{1/2}$ ) with a more rigorous method;
- iii) to compare the kinetic results obtained from different empirical equations for the transport term with those from the experimental value of activation energy for reptation;
- iv) to compare the values of fold surface energies obtained from the overall crystallization with those from direct determinations of crystal growth rates.

### 2. EXPERIMENTAL METHODS AND MATERIALS

The material chosen for this study was a commercial grade PET produced by EniChem Polimeri (Italy), free of opacifiants. The impurities present were the catalysts ( $\text{Sb}_2\text{O}_3$  and Manganese Acetate) and residual Diethylene Glycol ( $\sim 2.0-2.5\%$ ).

The intrinsic viscosity was  $[\eta] = 0.62$ , corresponding to a number average molecular

weight  $\langle M_n \rangle = 19,600$ . The zero frequency melt viscosity was determined between 245 and 290°C after melting at 300°C for 2 minutes, with a Rheometrics Mechanical Analyzer. Our specimens exhibit Newtonian behavior up to ~ 1 rad/s.

The hot stage microscopy work was carried out in a Mettler HSM microscope, coupled with photosensitive diode in the eyepiece. The 10-20  $\mu_m$  specimens were melted at 283°C for 5 min, quenched at ~100°C/min (under N<sub>2</sub> flow) to the desired temperature and treated for times long enough to saturate the light depolarization signal.

The DSC experiments were carried out in a Perkin-Elmer DSC-7 in N<sub>2</sub> flow. The temperatures and heat flux were calibrated with high purity standards. The isothermal crystallization experiments were performed after melting at 300°C for 1min and quenching at 100°C/min to the treatment temperature.

### 3. RESULTS and ANALYSES

In this section we analyze quantitatively the kinetics from the HSM and DSC studies in the framework of the theories of crystal growth and overall crystallization, summarized elsewhere [13]. First we analyze the crystallization mechanism of our sample and then we test the effect of the experimental techniques and methods (HSM vs. DSC; intercepts vs.  $t_{1/2}$ ) as well as diffusion term (Williams-Landel-Ferry vs. Hoffman approximations vs. experimental values of the transport term) used in the analyses, on the values of the fold surface energy,  $\sigma_e$ , calculated from the overall crystallization rates. Finally, we compare these values of surface energies with those determined by direct measurements of growth rates.

#### The crystallization mechanism

A limiting case of the possible nucleation mechanisms is easily modeled, i.e. **instantaneous heterogeneous nucleation** from a fixed number of sites (N) followed by bidimensional growth. In this case, the fractional volume transformed X is given by:

$$X = 1 - \exp(-\pi \cdot N \cdot G^2 \cdot t^2) \quad (1)$$

where G is the growth rate and t the time. Thus a plot of  $\ln \ln (1-X)^{-1}$  vs.  $\ln(t)$  should

give a straight line with slope 2 and intercept  $\ln(\pi N G^2)$ . The Avrami plots for both HSM and DSC yielded reasonable good (parallel) straight lines up to X = 70-90 %, with n ~ 2. The intercept (and thus the kinetics) decreased significantly with  $190 < T_c < 245$  °C. In the thin films used in the HSM study, two-dimensional growth of circular spherulites was forced to occur and hence n should be 2. In the DSC study, however, bulkier specimens (10 mg) than those of the HSM study (0.1 mg) were used, and thus tridimensional growth could have been more significant, which should give n=3. However, DSC detects the evolution of heat from the growing two-dimensional (lath shaped) lamellae, which constitute the spherulites, and thus n = 2.

Additionally, the  $t_{1/2}$  and crystal growth curves, for a number of PET specimens from different sources, show a surprising coincidence for the temperature of fastest kinetics (175- 180°C), in a clear indication that the overall crystallization of PET is controlled mainly by growth, rather than by primary nucleation. In conclusion, fast heterogeneous nucleation followed by spherulitic growth is the dominating mechanism in our polymer.

#### Comparison between different methods of kinetic analyses

Assuming that the controlling mechanism is two-dimensional secondary nucleation at the crystal/supercooled liquid interface, the equation for crystal growth reads [13]:

$$G = G_0 \exp(-E_d/RT) \exp(-K_g / T \cdot \Delta T \cdot f) \quad (2)$$

where  $G_0$  is a constant and  $E_d$  is the activation energy for segmental transport at the interface. The thermodynamic term,  $K_g = 2b_0 \cdot \sigma \cdot \sigma_e \cdot T_m^0 \cdot V_m / k \Delta H_m$ , where  $b_0$  is the new layer thickness,  $\sigma$  and  $\sigma_e$  the lateral and fold surface energies, respectively,  $T_m^0$  the equilibrium melting point,  $V_m$  the molar volume and  $\Delta H_m$  the molar heat of melting. Equation (2) applies for crystallization regime II, while for regimes I and III,  $K_g$  is twice that value. The lateral surface free energy  $\sigma$  usually varies from 5 to 20 mJ/m<sup>2</sup>.

Our next objective is to estimate and

compare the surface energies from the overall crystallization kinetics, carried out here by different experimental techniques and methods of analyses, with surface energies calculated from direct determinations of crystal nucleation and growth rates. Unfortunately, due to the copious nucleation and, consequently, extremely small spherulite sizes in our specimens, it was not possible to measure directly the crystal nucleation and growth rates and thus we use crystal growth data reported in the literature.

In our case, the Avrami intercept is:  $\text{int} = \ln(\pi N G_o^2)$ , which combined with the growth rate expression (2) leads to:

$$\text{int}/2 + E_d/RT = K'' - K_g / (T \cdot \Delta T \cdot f) \quad (3)$$

where  $K'' = \ln(\pi \cdot N \cdot G_o^2)/2$ . If  $N$  does not vary with temperature, a plot of  $\text{int}/2 + E_d/RT$  vs.  $1/(T \cdot \Delta T \cdot f)$  should be a straight line, from which one can estimate the product of the surface energies from the slope and  $N \cdot G_o^2$  from the intercept. If  $N$  varies with temperature the plots will not be straight. By an analogous rationale, it can be shown that:

$$\ln(1/t^{1/2}) + E_d/RT = K''' - K_g / (T \cdot \Delta T \cdot f) \quad (4)$$

The transport term and comparison with literature values

An important problem in the kinetic analyses of polymer crystallization is the determination of the transport term of Equation (2). The first approach is to use the "universal" constants, proposed long ago by Williams, Landel and Ferry [14]:

$$E_{wlf} / RT = 17230 T / R(51.6 + T - T_g)^2 \quad (5)$$

More recently, Hoffman et al. [13] demonstrated that an empirical expression of the form:

$$E_h / RT = U^* / R(T - T_g - 30) \quad (6)$$

where  $U^*$  varies between 4200 and 6700 J/mole, can fit very well the growth rate data for several polymers, when used with Equation (2).

Finally, one can use the experimental value of the "zero shear" viscosity of the undercooled melt in the temperature range of interest to calculate directly the activation

energy for reptation ( $E_{ex}$ ), which is then assumed to be equal to that for segmental transport at the interface. In our case, the apparent activation energy was 66 kJ/mole between 245 C and 290°C, hence,

$$E_{ex} / RT = 7970 / T \quad (7)$$

Figure 1 shows plots for the HSM data, based on the Avrami intercepts, using Equation (3) with the three expressions (5-7) for the transport term. Figure 2 shows analogous plots for the DSC experiments. Although they are not perfect straight lines, indicating a probable variation of  $N$  with temperature, we performed linear regression analysis to estimate "average" surface energies.

Table 1 summarizes the values of the constants ( $\ln(\pi \cdot N \cdot G_o^2)/2$ ), the calculated surface energies and the correlation coefficients calculated from those figures.

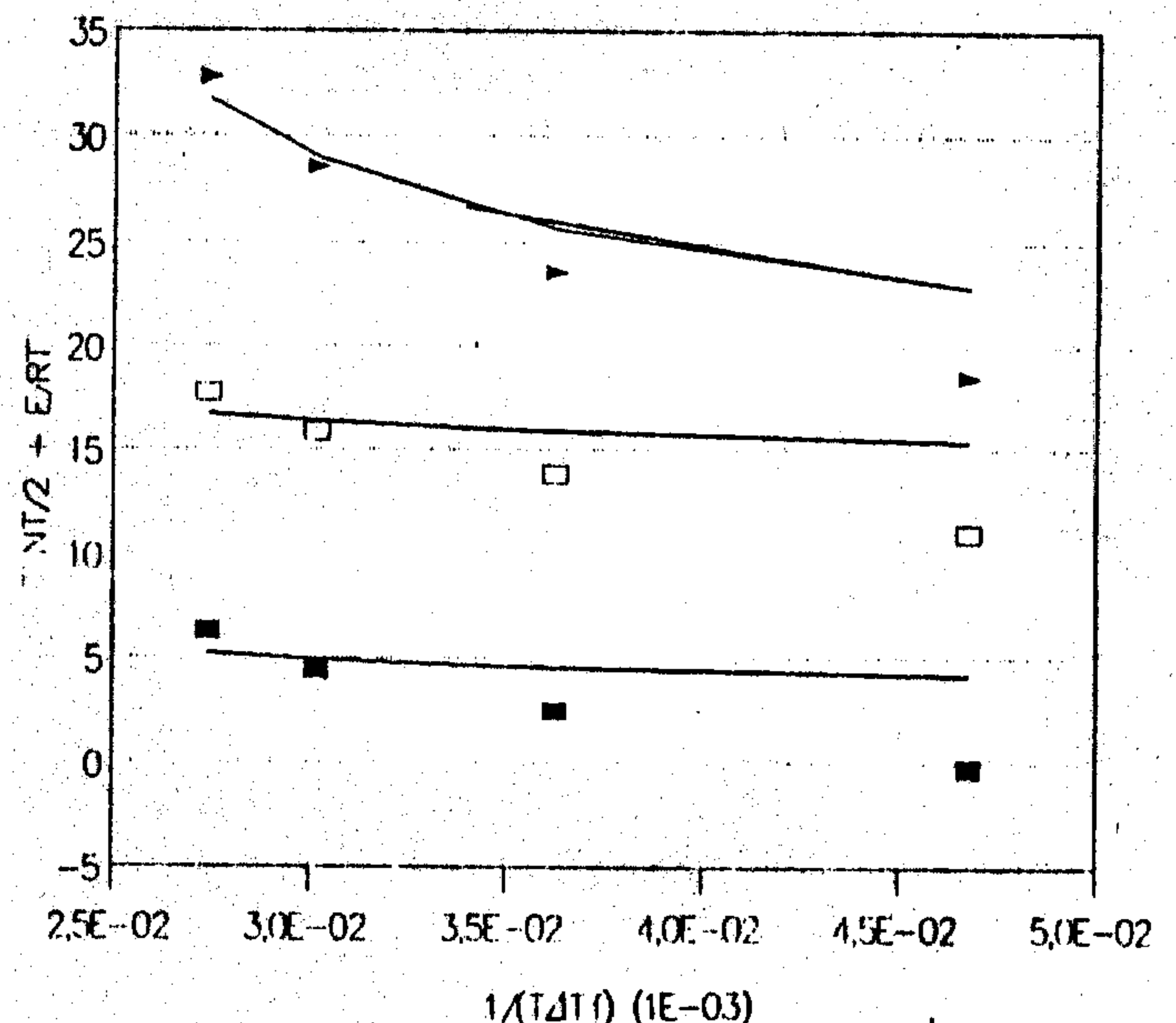


Figure 1.  $\text{Int}/2 + E_d/RT$  vs.  $1/T \cdot \Delta T \cdot f$  plots for the HSM data. (■) Hoffman approximation; (□) Experimental  $E_d$ ; (▴) WLF approximation. The solid lines refer to the values of  $E_d/RT$  calculated by Eqs. (6), (7) and (5), for the Hoffman, Exp. and WLF, respectively.

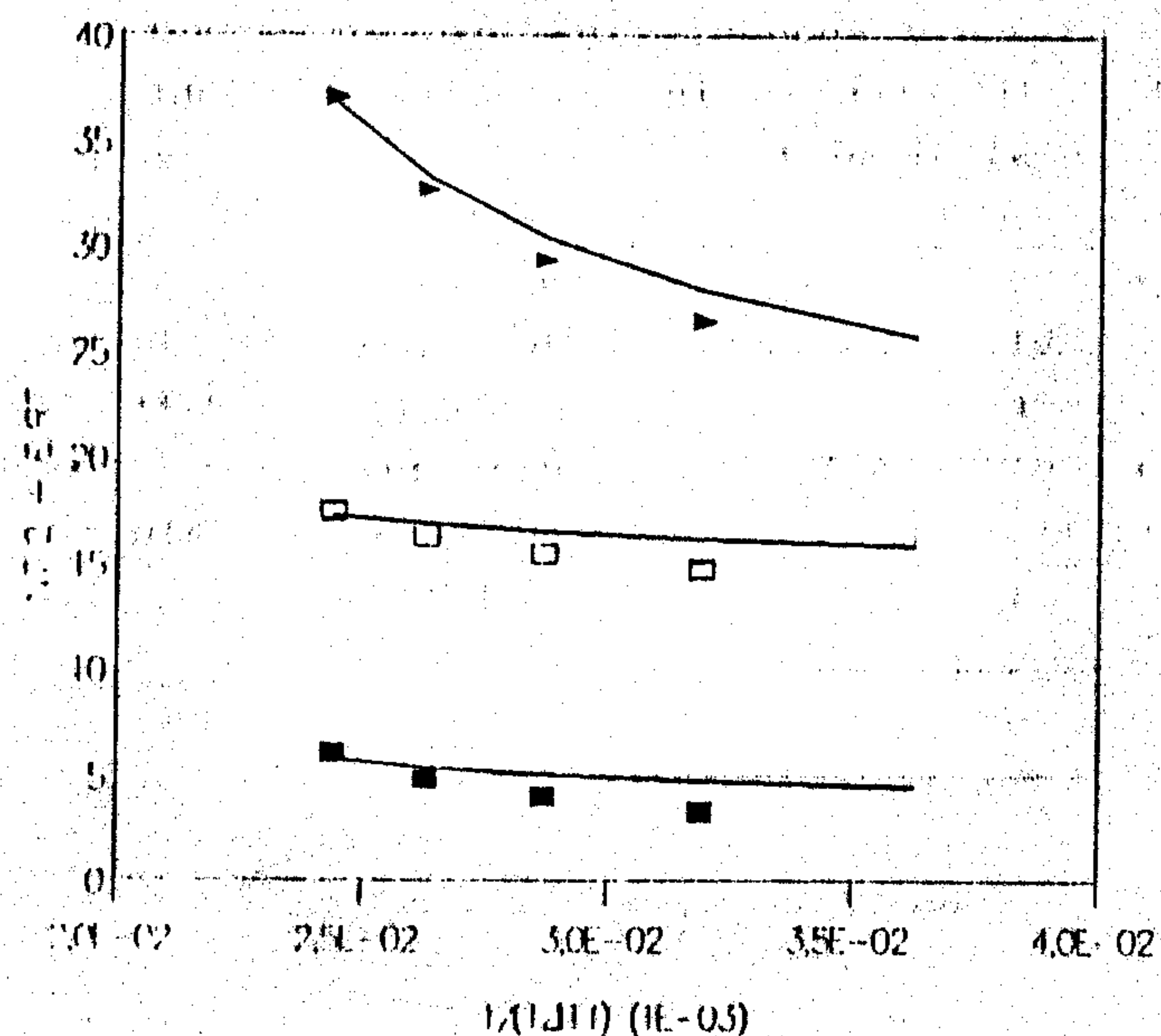


Figure 2.  $\text{Int}/2 + E_d/RT$  vs.  $1/T \cdot \Delta T \cdot f$  for the DSC data. The symbols are the same as in Fig. 1.

Table 1. Crystallization parameters for different approximations of the transport term

Transport	cte		$\sigma_e$ (mJ/m <sup>2</sup> )		$r^2$	
	4	3	4	3	4	3
<b>Hot Stage Microscopy</b>						
WLF	51-46		320-270		0.950-0.980	
Hoff	14-13		145-126		0.969-0.996	
Exp	26-25		150-130		0.970-0.996	
<b>Differential Scanning Calorimetry</b>						
WLF	70-61		630-500		0.971-0.988	
Hoff	15-12		161-119		0.957-0.984	
Exp	26-23		163-123		0.962-0.987	

\*The two values for each parameter refer to regression analyses with all four data points and with only the last three points.

In the calculation of  $\sigma_e$  it was assumed that  $\sigma$  is given by the Thomas-Stavely relation, i.e.  $\sim 10 \text{ mJ/m}^2$ , and the crystallization regime is II, with the following parameters:

$\Delta H_m = 140 \text{ J/g}$ ,  $T_m^0 = 561 \text{ K}$ ,  $T_g = 318-323 \text{ K}$ ,  
 $[M] = 0.192 \text{ kg}$ ,  $V_m = 1.32 \cdot 10^{-4} \text{ m}^3/\text{mole}$ ,  
 and  $b_0 = 5.53 \cdot 10^{-10} \text{ m}$ .

The values of  $N \cdot G_0^2$  and  $\sigma_e$  resulting from the WLF approximation for the transport term are much higher than those from the other two equations. However, there is good agreement between the estimates resulting from the use of the empirical equation of Hoffman and from the experimental value of  $E_d$ , by both HSM and DSC. The fold surface energy is between 130-145 mJ/m<sup>2</sup> for the HSM study and 120-160 mJ/m<sup>2</sup> for the DSC experiments. These values are well within the range reported for other polymers.

#### Comparison with literature values

As far as we know there is no previous quantitative report on the overall crystallization of PET, as measured by the Avrami intercepts, with a constant  $n$  ( $n$  varied with temperature in all papers reviewed), so we cannot compare our "intercepts" results with literature data. It is possible, however, to compare the kinetic parameters obtained from the "intercepts" method with the approximate kinetics determined by  $1/t_{1/2}$  in this study, as well as from published data for  $t_{1/2}$ , and for spherulitic growth rates.

Spherulite growth rates have been determined in extensive temperature ranges (through  $G_{\text{max}}$ ) by Antwerpen and Krevelen [10] for PETs, with a range of molecular weights,  $19,000 < M_n < 39,000$  (measured after crystallization). Phillips et al. [11-12] also determined the growth rates of PETs with  $\langle M_n^i \rangle = 21,000$  and  $19,000$  (initial MW, before melting and crystallization), containing 0.7 % residual diethylene glycol. The surface energies calculated from these data are given in Table 2. For comparison purposes,  $T_g = 323 \text{ K}$  and  $U^* = 6,700 \text{ J/mole}$  were used in the Hoffman expression (Eqs. 2 and 6). The plots were made as a function of  $1/(T \cdot \Delta T \cdot f)$  to allow for the wide range of undercoolings covered, specially in the crystal growth experiments.

Table 2. Kinetic parameters for regime II crystallization (regression with all points).

Method	cte*	$\sigma_e$ (mJ/m <sup>2</sup> )	r <sup>2</sup>
<b>Overall crystallization</b>			
DSC int	15	161	0.957
HSM int	14	145	0.967
DSC t <sub>1/2</sub>	10	151	0.998
HSM t <sub>1/2</sub>	12	155	0.935
Cobbs t <sub>1/2</sub>	4	118	0.983
<b>Growth rates</b>			
G Phi 19	-0.9	185	0.999
G Phi 21	+1.8	203 (142)**	0.999
G Ant 19	-2.0	151 (152)**	0.999
G Ant 39	-1.5	195 (219)**	0.993

\* cte =  $\ln(\pi N G_o^2)/2$  for the "int/2" plots;  $\ln(\pi N G_o^2 / \ln 2)/2$  for "ln(1/t<sub>1/2</sub>)" plots;  $\ln(G_o)$  for the G data.

\*\*values between brackets refer to regime III

Table 2 shows that the surface energies determined here from the overall crystallization kinetics, for a PET of  $\langle M_n^i \rangle = 19,600$  (initial MW), by the combination of techniques (DSC, HSM, int or t<sub>1/2</sub>), vary from 145 to 160 mJ/m<sup>2</sup> (int) and from 150 to 155 mJ/m<sup>2</sup> (t<sub>1/2</sub>). These values are higher than 118 mJ/m<sup>2</sup>, calculated from the IR data of Cobbs and Burton [2]. However, they agree very well with those from the growth rate study of Antwerpen and Krevelen [10] for a PET of  $\langle M_n \rangle = 19,000$ , being substantially smaller than the values calculated for a PET with  $\langle M_n \rangle = 39,000$ , and than those from the studies of Phillips et al [11, 12] for PETs of  $\langle M_n^i \rangle = 19,000$  and 21,000 (data for crystallization regime II). On the other hand, our results agree quite well with the values calculated for the data corresponding to regime III. As  $\sigma_e$  should not depend on the crystallization regime, these last values (for regime III) are believed to be more accurate because they are compatible with ours and with those of [10], for polymers of similar molecular weights.

As demonstrated here,  $\sigma_e$  does not depend strongly on the experimental technique used (similar DSC and HSM values with int or with t<sub>1/2</sub>), thus the differences between ours and some literature values of surface energy

immediately suggests that the main factor is the difference in molecular weight and residual impurities among the several samples used in distinct studies. However, it should be stressed that different values of U\* should probably be used in the analyses of each polymer, in order to account for the different molecular mobility. This procedure could minimize the divergence between the values of  $\sigma_e$ , and will be discussed shortly.

The growth data of Antwerpen and Krevelen [10] for PET specimens with  $\langle M_n \rangle = 19,000$  and 39,000, produced from solid state polycondensation from the same batch, and thus containing the same catalysts and residual DEG, provide a way to test the effect of E<sub>d</sub> on  $\sigma_e$ . In order to force the fold surface energy of the 39,000 polymer (195 mJ/m<sup>2</sup>; r<sup>2</sup> = 0.993) to equalize that of the low MW specimen (151 mJ/m<sup>2</sup>), it is necessary to impose a much lower value for U\*/R instead of 806 (used in the analyses), however, that significantly decreases the correlation coefficient r<sup>2</sup>. Actually, the only way to optimize the fit quality was to input a value of 900 for U\*/R, which improved the fit very little (r<sup>2</sup> = 0.994) but lead to a even higher value of surface energy,  $\sigma_e = 216$  mJ/m<sup>2</sup>, increasing the difference between the low and high MW polymers. Thus, the MW dependence of  $\sigma_e$  is clear, and explains the differences of Table 2 between ours and some literature values.

In summary, taken into account the difficulties resulting from: i) the unknown value of MW (after melting and crystallization which may produce different levels of regradation); ii) the right choice of E<sub>d</sub> for each polymer and iii) the probable variation of N with temperature, previously mentioned, the values of  $\sigma_e$  calculated from the overall crystallization kinetics study performed here (145-160 mJ/m<sup>2</sup>, from the Avrami intercepts, and 150-155 mJ/m<sup>2</sup> from ln(1/t<sub>1/2</sub>) plots) compare reasonably well with those from literature data for spherulitic growth rates in PET (140 <  $\sigma_e$  < 200 mJ/m<sup>2</sup>). The difference can be easily accounted for by the differences in MW between the polymers used in the distinct studies.

#### 4. CONCLUSIONS

The analyses of the experimental studies carried out here combined with literature data allow the following conclusions to be drawn:

- i) The crystallization mechanism of our PET was clearly instantaneous heterogeneous nucleation from a great number of active sites. Hence, the overall crystallization rate was controlled mainly by spherulitic growth;
- ii) The DSC and HSM results were in substantial agreement for both the Avrami coefficient ( $n=2$ ) and crystallization kinetics;
- iii) Good agreement was also found for the kinetic results from the approximate ( $t_{1/2}$ ) and from the more rigorous (Avrami intercepts) methods;
- iv) The effect of the transport term on the kinetic results was tested. It was shown that the WLF approximation gives too high values of surface energies. On the other hand, the empirical expression of Hoffman gave results quite close to those from the experimental values of activation energy for viscous flow. This vindicates the use of the Hoffman equation, when experimental data are not available, and suggests that the diffusion mechanism involved in crystallization is related to macroscopic flow;
- v) The fold surface energy values estimated from the overall crystallization kinetics ( $145-160 \text{ mJ/m}^2$ ) with a combination of techniques (DSC, HSM,  $t_{1/2}$  or Avrami int.), using the Hoffman expression for diffusion, compare well to those calculated from literature data for spherulitic growth rates ( $140-200 \text{ mJ/m}^2$ ). The difference with some literature values can be accounted for by the molecular weights differences between the specimens used in the several studies.

#### ACKNOWLEDGEMENTS

The authors thank the valuable help of Drs. T. Simonazzi, F. Sevini, G. Paganetto and of M. Cappati, G. Artioli and O. Blo and M. Gabaldi, from Himont, and the critical review of prof. G. Alfonso. Financial support by the Montecatini Group (Italy) and by RHA/E/UFSCar (Brazil) is appreciated.

#### REFERENCES

1. Kolb, H.J. and Izard, E.F.- J. Applied Phys., 20 (1949) 571-579.
2. Cobbs Jr., W.H and Burton, R.L.- J. Polym. Sci., X(3), (1952) 275-290.
3. Keller, A.; Lester, G.R. and Morgan, L.B.- Philos. Trans. Roy. Soc. London, Ser.A, 247 (1954) 1-8.
4. Misuishi, Y. and Ikeda, J. Polym. Sci.4, Part A2 (1966) 283-289.
5. Fielding-Russell, G.S. and Pillai, P.S.-Die Makrom. Chem.,135 (1970) 263-274.
6. Groeninckx, G. et al.- J. Polym. Sci.(Phys.),12 (1974) 303-316.
7. Jackson, J.B and Longman, G.W.- Polymer, 10 (1969) 873-878.
8. Mayhan, K.G.; James, W.J. and Bosch, W.- J. Appl. Polym. Sci.,9 (1965) 3605-3616.
9. Collier, J.R. and Baer, E.- J. Appl. Polym. Sci.,10 (1966) 1409-1419.
10. Van Antwerpen, F. and Van Krevelen, D.W.- J. Polym. Sci. (Phys.-A2), 10 (1972) 2423-2434.
11. Paly, L. and Phillips, P.J.- J. Polym. Sci.(Phys.), 18 (1980) 829-842.
12. Phillips, P.J. and Tseng, H.T.- Macromolecules, 22 (1989) 1649-1655.
13. Hoffman, J. D.; Davies, G.T. and Lauritzen, J.I- in "Solid State Chemistry" Plenum Press, new York, vol. 3, chap. 7, (1976) 497-614.
14. Williams, M.L; Landel, R.F. and Ferry, J.H.- J. Am. Chem. Soc., 77, (1955)3701-3710